TUDelft

Delft University of Technology

Validation of engineering dynamic inflow models by experimental and numerical approaches

Yu, Wei; Hong, V.W.; Simao Ferreira, Carlos; van Kuik, Gijs

Citation (APA)
Yu, W., Hong, V. W., Simao Ferreira, C., & van Kuik, G. (2016). Validation of engineering dynamic inflow models by experimental and numerical approaches. *Journal of Physics: Conference Series*, *753*. https://doi.org/10.1088/1742-6596/753/2/022024

Important note
To cite this publication, please use the final published version (if applicable).
Please check the document version above.

Validation of engineering dynamic inflow models by experimental and numerical approaches

W. Yu, V.W. Hong, C. Ferreira and G.A.M. van Kuik

Faculty of Aerospace Engineering, Delft University of Technology, Kluyverweg 1, 2629 HS, Delft, The Netherlands

E-mail: `W.Yu@tudelft.nl`

Abstract.

The state of the art engineering dynamic inflow models of Pitt-Peters, Øye and ECN have been used to correct Blade Element Momentum theory for unsteady load prediction of a wind turbine for two decades. However, their accuracy is unknown. This paper is to benchmark the performance of these engineering models by experimental and numerical methods. The experimental load and flow measurements of an unsteady actuator disc were performed in the Open Jet Facility at Delft University of Technology. The unsteady load was generated by a ramp-type variation of porosity of the disc. A Reynolds Averaged Navier-Stokes (RANS) model, a Free Wake Vortex Ring (FWVR) model and a Vortex Tube Model (VTM) simulate the same transient load changes. The velocity field obtained from the experimental and numerical methods are compared with the engineering dynamic inflow models. Velocity comparison aft the disc between the experimental and numerical methods shows the numerical models of RANS and FWVR model are capable to predict the velocity transient behaviour during transient disc loading. Velocity comparison at the disc between the engineering models and the numerical methods further shows that the engineering models predict much faster velocity decay, which implies the need for more advanced or better tuned dynamic inflow models.

1. Introduction and Objective

A wind turbine operates in a highly dynamic state. The currently most popular design theory of wind turbine — BEM, is based on the assumption of quasi-steady state. The steady assumption made in BEM is at two levels, unsteady airfoil aerodynamics, and unsteady wake in the momentum theory. The latter is the commonly called 'Dynamic Inflow'. The current approaches to overcome the limitation of quasi-steady wake assumption made in BEM is to use engineering dynamic inflow models. Different dynamic inflow models have been proposed [1]. These dynamic inflow models have been compared with experiments for rotors with finite number of blades by Snel and Schepers [1], Schepers and Snel [2] and the test of Unsteady Aerodynamic Experiments in the NASA Ames tunnel [3]. A CFD model was developed for unsteady rotor aerodynamics by Sørensen and Kock [4], the calculated blade flapping moment was in close agreement with experimental results for step blade pitch of 2MW Tjæreborg wind turbine. Good agreement with the latter experiment [3] for low loading case was achieved using BEM coupling with tuned time constants, which were tuned by solving RANS equations [5].

These researches focused on the dynamic inflow on a wind turbine rotor with a finite number of blades. Scarce published record exists on the experimental use of actuator discs under unsteady

loading to investigate the phenomena. The use of an actuator disc to investigate the dynamic inflow effects is of interest as it is the basis of BEM as well as engineering dynamic inflow models of Pitt-Peters [6], Øye [7] ,[8], and ECN [9].

A free wake vortex ring model which accounts for the induced velocity field of any non-uniform and unsteady loaded actuator disc was developed by Yu *et al* [10]. The steady classical actuator disc model was also extended to arbitrary non-uniform and unsteady axi-symmetrical disc loads in [11]. Discrepancy of engineering dynamic inflow models of Øye and Pitt-Peters from these models in predicting the transient induction at the disc of a wind turbine rotor has been shown [10, 11].

The objective of this paper is to validate and benchmark the state of the art dynamic inflow models of Pitt-Peters [6], Øye [7, 8], and ECN [9] against experimental and numerical methods.

2. Method
2.1. Engineering dynamic inflow models
 (i) The Pitt-Peters dynamic inflow model

   The Pitt-Peters dynamic inflow model [6] was developed for an actuator disc with an assumed inflow distribution across the disc. Based on the assumption that the equation of Pitt-Peters can be applied to a blade element or actuator annulus level, the dynamic inflow equation for each annular ring becomes

$$\frac{1}{\rho A_j V_0^2/2} \left[\frac{8}{3\pi} \rho A_j r_j \frac{dv_j}{dt} + 2\rho A_j v_j (V_0 + v_j) \right] = C_{tj} \tag{1}$$

   where j indicates the jth annular ring, A_j and C_{tj} are the area and thrust coefficient of the jth annulus and v_j is its azimuthal averaged induced velocity.

 (ii) The Øye dynamic inflow model

   In the Øye dynamic inflow model [7, 8], the induced velocity is estimated by filtering the quasi-steady values through two first-order differential equations

$$v_{int} + \tau_1 \frac{dv_{int}}{dt} = v_{qs} + b\tau_1 \frac{dv_{qs}}{dt} \tag{2}$$

$$v_z + \tau_2 \frac{dv_z}{dt} = v_{int} \tag{3}$$

   where v_{qs} is the quasi-steady value from BEM, v_{int} is an intermediate value and the final filtered value v_z is treated as the induced velocity. After calibration using a vortex ring model [8], the two time constants are recommended as follows [1]

$$\tau_1 = \frac{1.1}{(1 - 1.3a)} \frac{R}{V_0} \tag{4}$$

$$\tau_2 = (0.39 - 0.26(\frac{r_j}{R})^2)\tau_1 \tag{5}$$

   where a is the axial induction factor, R is the rotor radius, r_j is the radius of jth annulus, and b is a constant value of 0.6.

 (iii) The ECN's dynamic inflow model

   The dynamic inflow model developed by ECN [9], was derived from an integral relation of the stream tube model (see more details of the streamtube model in [12]). For the condition of constant wind speed, the equation is

$$\frac{R}{V_w} f_a \frac{da}{dt} + a(1 - a) = C_{tj}/4 \tag{6}$$

where C_{tj} is the axial force coefficient on the rotor annulus j. The term f_a is a function of the radial position, defined as

$$f_a = 2\pi / \int_0^{2\pi} \frac{[1 - (r/R)cos\Phi_r]}{[1 + (r/R)^2 - 2(r/R)cos\Phi_r]^3/2} d\Phi_r \qquad (7)$$

2.2. Validation Methods

The performance of engineering models of Pitt-Peters, Øye and ECN will be benchmarked against the results from

- experiments of an unsteady actuator disc model
- a linear Vortex Tube Model
- a Free Wake Vortex Ring model
- a RANS simulation

The experiments were carried out in the low speed closed-circuit Open Jet Facility (OJF) located at the Delft University of Technology. The OJF wind tunnel has an octagonal cross-section of 2.85×2.85 m^2 and a contraction ratio of 3:1. It is free to expand in an area of $13.7 \times 6.6 \times 8.2$ m^3. The free stream velocity ranges from 3 m/s to 34 m/s with a flow uniformity of 0.5% and a turbulence level of 0.24%, powered by a 500 kW electric motor. The temperature in the test section is maintained at a constant temperature of 20°C by a 350 kW heat exchanger throughout the experiments. The tested wind speed for this experiment is 6 m/s. The set-up is given in Figure 1(a). A hot-wire probe is mounted on a transverse system, which can transport the probe axially and radially to the desired measurement points.

In this experiment, the loading on the disc was changed by adjusting the relative open area (porosity) formed by two identical parallel porous discs. The two identical discs are made from 2.0 mm thick aluminium plate with punctured 10×10 mm^2 square holes. Each disc has a diameter of 600 mm, hole-to-hole spacing of 2.0 mm, and porosity of 69.4%. The porous disc is shown in figure 1(b).

The porosity of the disc is changing in a ramp type profile (see Figure 2), with δt representing the ramp time. The reduced ramp time s is used here. s is defined by

$$s = \frac{1}{D} \int_0^{\delta t} V_0 dt \qquad (8)$$

which represents the relative distance travelled by the flow in terms of the diameter of the actuator disc during the time interval δt. Different reduced ramp time cases were tested.

The thrust was measured using a load cell mounted between the tower and the disc model. The flow downstream of the disc was measured at various positions using hot-wire anemometry. The two vortex models [10, 11] are used for the benchmark study. A RANS model also simulates the tested unsteady load cases. The description of these three numerical models will be introduced in the Appendix.

Notably, the engineering dynamic inflow models of Pitt-Peters, Øye and ECN can only predict the induction at the actuator plane. Even if it was practically possible to measure the velocity at the disc in this set-up, the accuracy of the measured velocity is still doubtful due to the effect of the small scale turbulent structures generated by the porous discs. For this reason, the comparison is done in two steps:

(i) The velocity from the experiments and the three numerical models of VTM, FWVR and RANS during transient disc load are compared at various locations aft the disc.

(ii) The velocity at the actuator disc from the three numerical models are then compared with that from the three engineering dynamic inflow models of Pitt-Peters, Øye and ECN for the same transient load change.
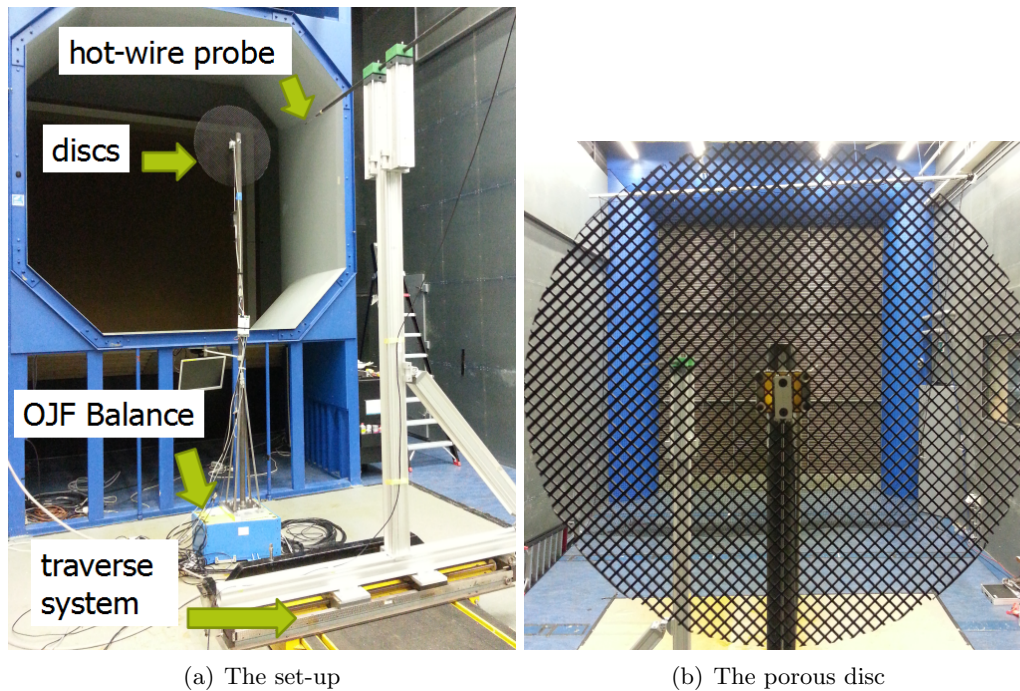
(a) The set-up

(b) The porous disc

Figure 1. The overview of experimental set-up in the wind tunnel and the tested porous disc
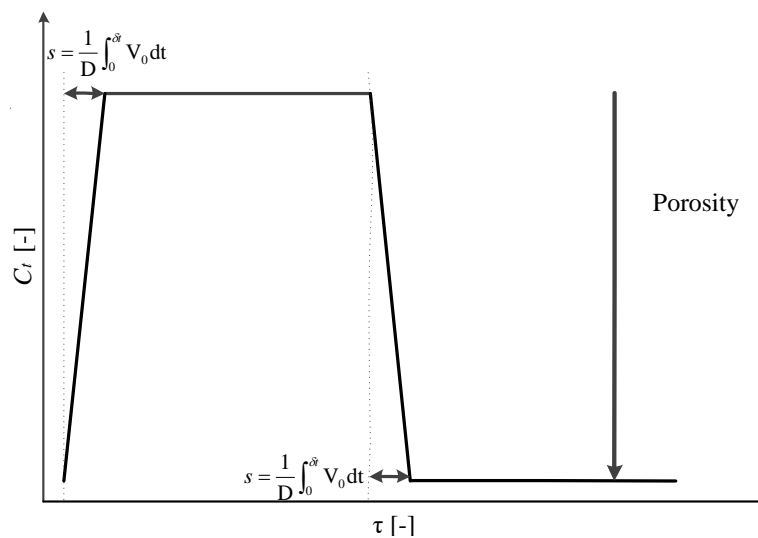

Figure 2. Unsteady load profile

3. Results and Discussion

Results of the case of reduced ramp time of 0.2 will be present here (more results are reffered to [13]). The diameter based Reynolds number is 270680. Knight [14] has shown that the aerodynamic thrust of an actuator disc is insensitive to Reynolds number when it is larger than 150000 using tunnel test of three different types of discs. Hoerner [15] summarized that above diameter-based Reynolds number of 1000, the drag coefficient of discs (and other plates) is practically constant up to the highest Reynolds numbers ever tested (approaching 10^7). Figure 3 gives the ensemble averaged thrust coefficient measured by the load cell. The dot line represents
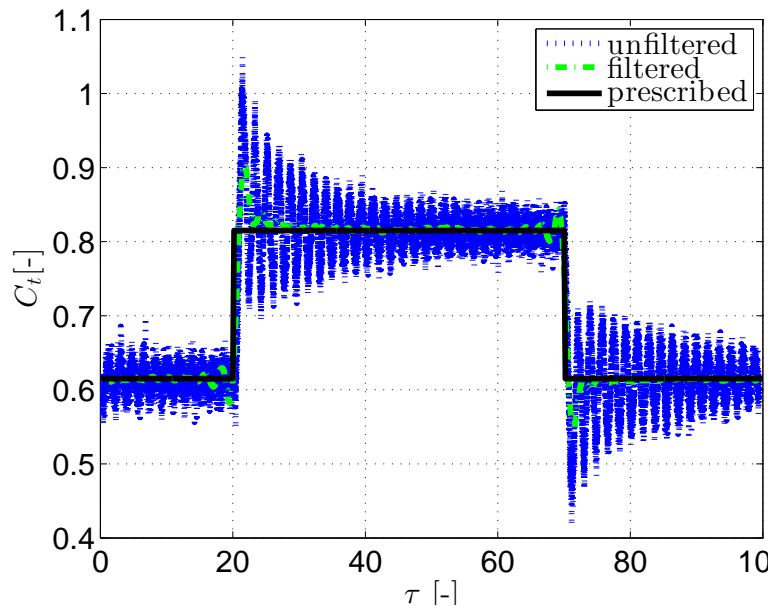
Figure 3. Thrust coefficient. dot and dash line: the ensemble averaged unfiltered and filtered C_t measured by the load cell, solid line: the prescribed C_t

the original acquired data. For the dash line, the system vibration frequency is filtered out from the raw data. The real transient time is affected by the dynamic response of the entire mechanical system. Thus, the same reduced ramp time as the porosity change of $s = 0.2$ is prescribed for the load change (plotted as solid lines), which serves as input for all the numerical models.

The velocity values are non-dimensionalised in the similar way as used in [1]. It is defined by the following equation

$$\widetilde{\Delta V_x} = \frac{V_x - V_{x,s1}}{V_{x,s2} - V_{x,s1}} \tag{9}$$

The subscripts $s1$ and $s2$ represent the initial (before load change) and the final steady state (sufficient time after load change). Hereinafter, the self-normalized transient response from all the methods are compared. The time given in this section is normalized by the characteristic time of dynamic inflow D/V_0.

Figure 4 presents the ensemble averaged velocity during the transient disc load at the inner wake y/D=0.33 for planes x/D=0.5,1.0,1.5,2.0,2.5,3.0. The ensemble averaged velocity during the unsteady load outside the wake at y/D=0.83 for the same six planes are shown in figure 5. The velocity from the experiments, RANS, FWVR model and VTM are compared. Due to the focus of this paper is the transient profile of velocity decay instead of the velocity overshoot and undershoot, which are observed in figure 4 and 5, it will be not discussed in detail. From figure 4 and 5, the VTM predicts rapid decay to the new steady state, which is faster than the velocity profiles from the other three methods. The velocity from the FWVR model matches that from the RANS model well, implying that the effect of the viscosity is not significant. Apart from some magnitude difference of the velocity overshoot and undershoot, the RANS and FWVR model can capture generally well the velocity transient change profiles from the experiment of an actuator disc undergoing unsteady load.

It is notable that the onset of responding time to the load variation from the FWVR and RANS model matches with the experimental results for all these measured planes. However, the further downstream the plane is, the earlier the VTM tends to start respond to the unsteady

5

load change. This is likely caused by the overestimation of the convection velocity of vortex element by the VTM.

The good agreement of velocity profiles at different downstream locations between the RANS, the FWVR model and the experiments shows that these numerical models are capable of predicting the transient velocity profiles of an actuator disc with unsteady loading.

Figure 6 compares the normalized averaged axial velocity at the actuator disc. The result from the Momentum Theory (MT) is also plotted for comparison. As seen, the engineering model of Pitt-Peters predicts fastest decay among all the methods. The velocity decay profiles predicted by the model of Øye, ECN and the VTM are very close. This is because all the three methods are developed based on the stream tube model. The velocity decay profiles predicted by all these three models are slower than that of Pitt-Peters model, but are still much faster than those from the other two more physically-representative numerical models, RANS and FWVR. The latter two models show good agreement with experiments in the velocity field aft the disc as shown above.
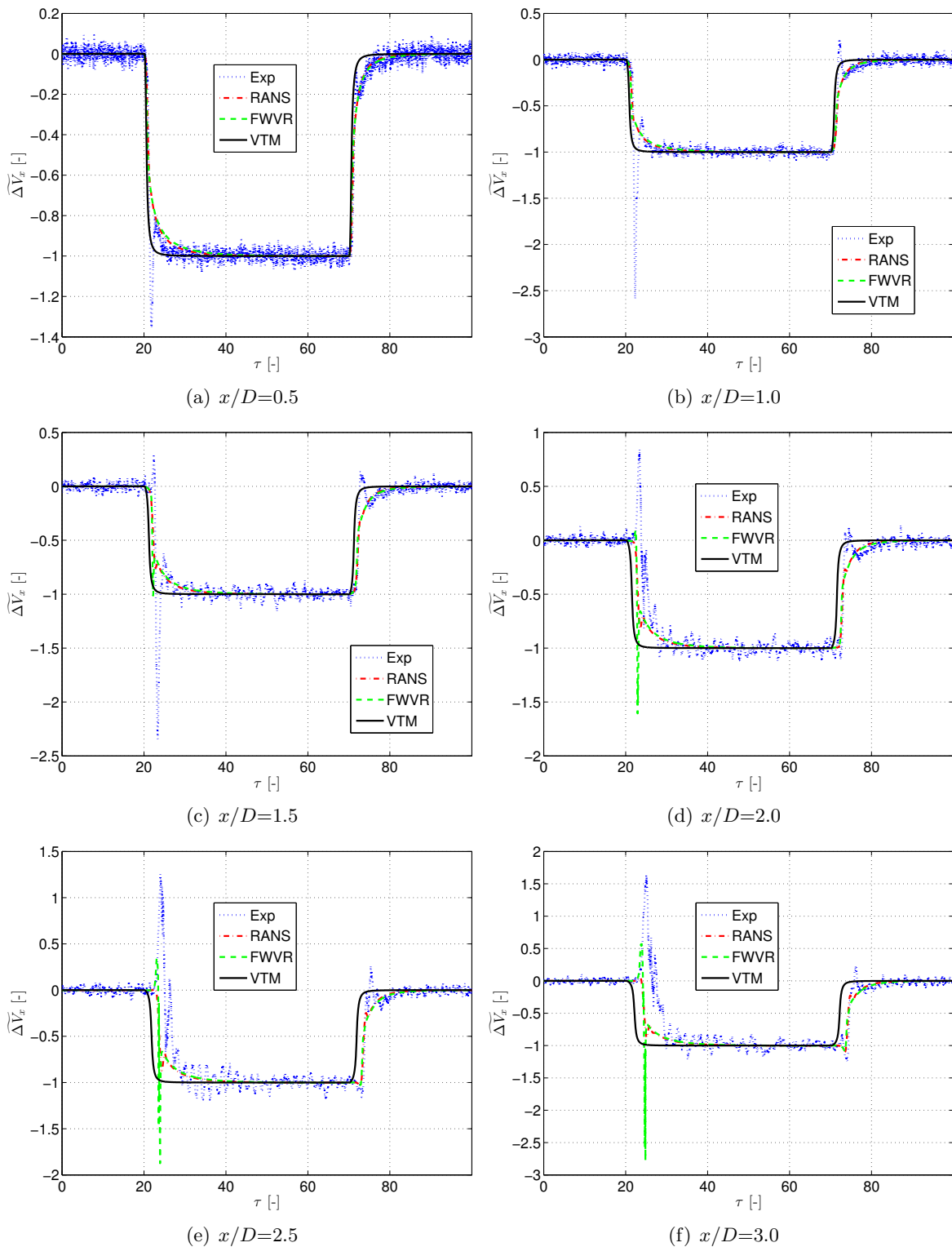
Figure 4. Ensemble averaged axial velocity in the inner wake at y/D=0.33 during transient load for planes x/D=0.5,1.0, 1.5, 2.0,2.5, 3.0. y : radial direction; x : axial direction
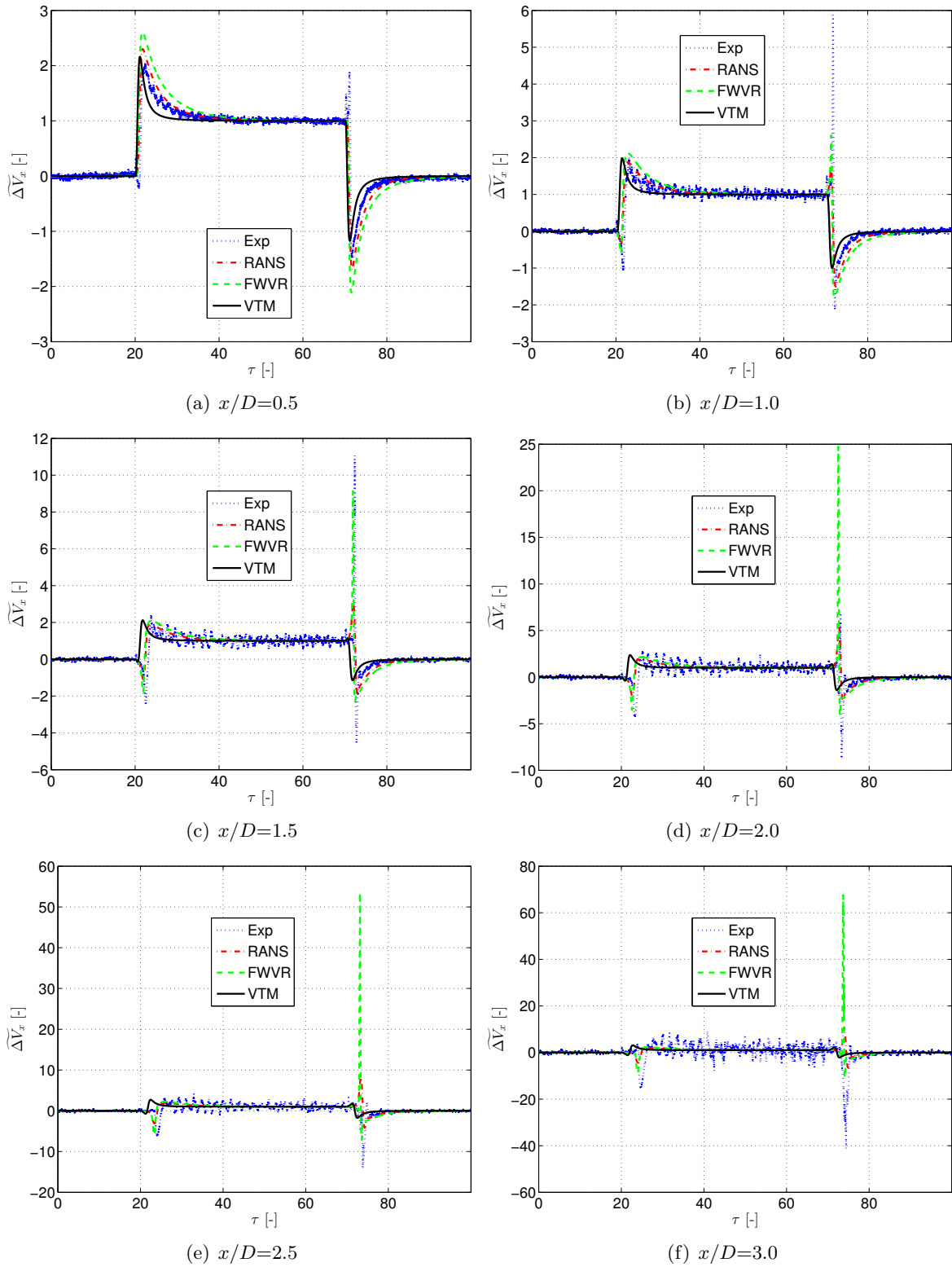
Figure 5. Ensemble averaged velocity outside the wake at y/D=0.83 during transient load for planes x/D=0.5, 1.0,1.5, 2.0, 2.5, 3.0. y : radial direction; x : axial direction
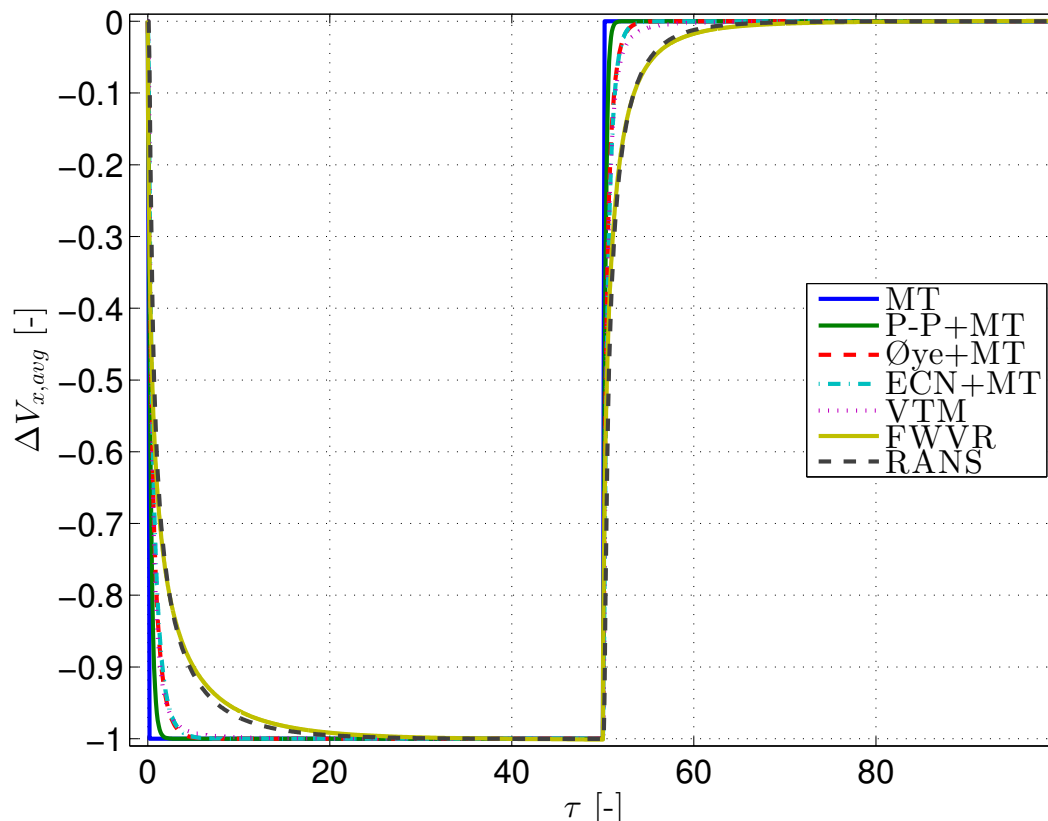
Figure 6. Normalized axial velocity at the actuator disc during transient load predicted by the MT, engineering models of Pitt-Peters, Øye and ECN, and the model of VTM, FWVR, RANS

4. Conclusion

The state of the art dynamic inflow models of Pitt-Peters, Øye and ECN are validated against experimental and numerical methods. The results show that the induction at the actuator disc predicted by the three engineering dynamic inflow models decays much faster than that from RANS, FWVR during transient load. Based on the good agreement in the induced velocity at different locations in the field predicted by the RANS, FWVR model and the experimental results, it can be inferred that the induction from the engineering models is also much faster than that from experiments. This shows the need for more advanced engineering dynamic inflow models, or better tuned of the existing ones which could be more universal for better prediction of flow response during dynamic loading.

Acknowledgments

References

[1] H. Snel and J. Schepers, "Joint investigation of dynamic inflow effects and implemention of an engineering method," tech. rep., Netherlands Energy Research Foundation ECN, 1995.
[2] J. Schepers and H. Snel, "Dynamic inflow: yawed conditions and partial span pitch control," tech. rep., Netherlands Energy Research Foundation ECN, 1995.
[3] M. Hand, D. Simms, L. Fingersh, D. Jager, J. Cotrell, S. Schreck, and S. Larwood, "Unsteady Aerodynamics Experiment Phase VI : Wind Tunnel Test Configurations and Available Data Campaigns," Tech. Rep. December, National Renewable Energy Laboratory, Colorado, 2001.

[4] J. Sørensen and C. Kock, "A model for unsteady rotor aerodynamics," *Journal of Wind Engineering and Industrial Aerodynamics*, vol. 58, pp. 259–275, 1995.

[5] N. N. Sørensen and H. A. Madsen, "Modelling of transient wind turbine loads during pitch motion," in *European Wind Energy Association (EWEA)*, (Brussels), 2006.

[6] D. Pitt and D. Peters, "Theoretical prediction of dynamic-inflow derivatives," *Vertica*, vol. 5, no. 1, pp. 21–34, 1981.

[7] S. Øye, "Unsteady wake effects caused by pitch-anlge changegs," in *Proceedings of the First IEA Symposium on the aerodynamics of wind turbines*, (London), 1986.

[8] S. Øye, "A simple vortex model of a turbine rotor," in *Proceedings of the third IEA symposium on the aerodynamics of wind turbines*, (Harwell), pp. 1–15, 1990.

[9] J. Schepers, *Engineering models in wind energy aerodynamics*. PhD thesis, 2012.

[10] W. Yu, C. Ferreira, G. van Kuik, and D. Baldacchino, "Verifying the Blade Element Momentum Method in unsteady, radially varied,axisymmetric loading using a vortex ring model," *Wind Energy.,doi:10.1002/we.2005*, 2016.

[11] W. Yu, C. Ferreira, and G. van Kuik, "Analytical actuator disk solution for unsteady and/or non-uniform loading," in *34th Wind Energy Symposium*, no. January, (California), pp. 1–12, 2016.

[12] M. O. L. Hansen, *Aerodynamics of wind turbines*. London: Earthscan. Second Edition, 2008.

[13] W. Yu, V. W. Hong, C. Ferreira, and G. van Kuik, "Experimental and numerical study of the dynamic wake of an unsteady actuator disc," *Journal of Fluid Mechanics, to be submitted*, 2016.

[14] Knight M, "Technical note NO. 253. — Wind tunnel standardization disk drag," tech. rep., National Advisory Committee for Aeronautics,Langley Aeronautical Laboratory, Washington, 1926.

[15] S. F. Hoerner, *Fluid-Dynamic Drag*. Hoerner Fluid Dynamics, 1965.

Appendix

4.1. The VTM model

The VTM [11] extends the classical steady cylindrical vortex tube model to unsteady flow. In this unsteady and radially uniform load case study, the vortex system is consisting of an infinite vortex tube and a number of finite vortex tubes, which are shed at different time steps when there is a load change on the actuator disc. The entire vortex system is convected downstream by the incoming flow and local induced velocity.

4.2. The FWVR model

In the free wake vortex ring model [10], the near wake is modelled by dynamic surfaces, consisting of free vortex rings shed from the edge of the actuator disc; the far wake is represented by a semi-infinite cylindrical vortex tube with constant strength and radius. The vortex rings are considered thin, axisymmetric and uniform. In this axisymmetric loaded actuator disc study, vortex rings may expand or contract, their central axis always coinciding with the axis of the actuator disc. A time step of $\Delta\tau = 0.02$ and a cut-off of $\delta = 1e - 5$ were chosen for the simulations after a convergence study.

4.3. The RANS model

The RANS equations are also solved. The turbulence model of $k - w$ Shear Stress Transport ($k - w$ SST) is used. The momentum sink represented by the actuator disc is introduced as a body force or source term in RANS. In this uniformly and axially loaded actuator disc study, source term is only added to the axial-direction momentum equation.

A mesh dependency study and a mesh density dependency study were carried out to determine the computation mesh size and cell size. The computation upstream, downstream and inlet sizes were chosen to be 10D, 30D and 30D respectively, each part is indicated in figure 7. The cell size of 0.5D and 0.083D were used for the Outside Wake and Wake regions respectively, as indicated in figure 7. For unsteady simulations, a 2nd order implicit temporal discretisation was used.
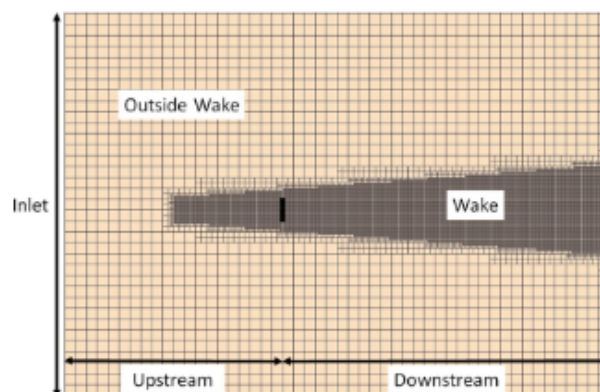

Figure 7. Planar side view of the Mesh of the computation domain